A comparative study of the interfacial roughness correlation and propagation in Mo/Si multilayers deposited using RF-magnetron sputtering on silicon, ule and zerodur substrates

2002 J. Phys.: Condens. Matter 14 8955

(http://iopscience.iop.org/0953-8984/14/39/305)

INSTITUTE OF PHYSICS PUBLISHING JOURNAL OF PHYSICS: CONDENSED MATTER

J. Phys.: Condens. Matter **14** (2002) 8955–8968 PII: S0953-8984(02)37736-1

A comparative study of the interfacial roughness correlation and propagation in Mo/Si multilayers deposited using RF-magnetron sputtering on silicon, ule and zerodur substrates

M Putero-Vuaroqueaux, H Faïk and B Vidal

L2MP-CNRS UMR6137, Faculté des Sciences de St Jérôme, case 131, 13397 Marseille Cedex 20, France

E-mail: magali.putero@l2mp.u-3mrs.fr, hasnaa.faik@l2mp.u-3mrs.fr and bernard.vidal@l2mp.u-3mrs.fr

Received 6 June 2002, in final form 1 August 2002
Published 19 September 2002
Online at stacks.iop.org/JPhysCM/14/8955

Abstract

Mo/Si multilayer (ML) mirrors play a decisive role in an extreme-ultraviolet (EUV) lithography process. In this study, the surface and interfacial roughness, as well as the lateral and vertical correlation lengths, of a series of Mo/Si MLs deposited by RF-magnetron sputtering (RF-MS) have been characterized using diffuse x-ray scattering and atomic force microscopy. We have investigated the influence of the substrate quality and material (silicon, ule and zerodur) on the propagation and the value of ML roughness. We show that, whatever the substrate is, the film deposited by RF-MS presents a reduced roughness compared with that of the substrate. Moreover, rocking-curve analyses show that, for Si and ule substrates, the ML average roughness is very low (<1.5 Å), associated with high spatial frequency oscillations, while in the case of zerodur substrates, the roughness is significantly increased (>2 Å), and the high spatial frequency oscillations are reduced. Finally, the combination of specular and non-specular small-angle x-ray results allows us to evaluate another key parameter, namely, the uncorrelated roughness which is an intrinsic characteristic related to the choice of both the deposition technique and the materials. This intrinsic roughness is found to be very low (2 Å) and constitutes a good argument in favour of the use of the RF-MS technique for EUV mirror deposition.

(Some figures in this article are in colour only in the electronic version)

1. Introduction

Extreme-ultraviolet (EUV) lithography using EUV light is the most promising next-generation lithography technology expected to realize patterning of device features in the range of 70–

30 nm [1, 2]. Most current designs of an EUV tool require several projection optical systems to reflect light in the wavelength range 11–14 nm at near normal angles of incidence in most cases [1, 3]. However, very few material combinations are known to result in multilayers (MLs) with high near-normal incidence reflectivity in the $\lambda < 30$ nm region. At a wavelength $\lambda = 13$–15 nm, the Mo/Si ML system represents a good material combination because of the high contrast between the optical constants of Si and Mo, and the low absorption of Si [4].

Therefore, the optics for EUV projection lithography consist of crystalline silicon or glass ceramic substrates, that can be flat or curved, coated with reflective Mo/Si ML films. The reflective mask blanks are made by patterning an absorber layer above the ML reflective coating [5].

The quality of the material structures and the features of the internal interfaces play a decisive role in achieving the optimum performance of MLs for EUV optics. Imperfections arise during the deposition process and are essentially due to intermixing and the reaction of Mo with Si. The roughness, which is in general defined as the standard deviation of the interface height, leads to non-specular scattering that has a drastic effect on image formation and resolution in the imaging system. In fact, non-specular scattering due to roughness decreases the useful throughput of the optical system and produces a background halo which reduces the contrast of the image [6]. For EUV optics, improvement of the image resolution via reduction of the roughness value (about less than 1 Å for the high spatial frequency roughness (HSFR)) is one of the main goals. For the reflective mask blanks, another property level is required together with high reflectivity: the lowest number of defects with a size of interest above 50 nm must be achieved on the ML reflective coatings [7–9]. Particles as small as 25 nm diameter on the reticular substrate have the potential to result in reticular film defects that could print on the wafer [10].

To minimize EUV ML mirror defects and roughness, high quality substrates are necessary. For instance, Mirkarimi *et al* [11] have shown that Mo/Si reflectance was a strong function of the substrate surface roughness. Furthermore, since the figure of the projection optics for an EUV lithography tool must be extremely precise to maintain resolution (see, for example, [1, 12]), it is also necessary to use substrates with a very low coefficient of thermal expansion in order to minimize thermal effects. Zerodur and ule glass-ceramic substrates are two strong candidates for EUV mirror substrates because of their extremely low thermal expansion coefficients [11–13].

In this study, Mo/Si MLs deposited using RF-magnetron sputtering (RF-MS) have been characterized, with special focus on the influence of the substrate type in terms of interfacial roughness and surface defects. Both small-angle x-ray reflectivity (SAXRR) and atomic force microscopy (AFM) have been used to characterize the MLs. The x-ray scattering technique particularly provides the possibility of non-destructive characterization of the internal interfaces. In this paper, we use x-ray reflectivity (XRR) and interface diffuse scattering analysis at grazing incidence to make a comparative study of the interface quality within MLs prepared by RF-MS on three different substrates (silicon, ule and zerodur). The influence of the deposition process and the substrate type on the correlated and uncorrelated interface roughness is discussed.

2. Experimental procedure and data analysis

2.1. Multilayer deposition

Mo/Si layer films were deposited using RF-MS [14]. The base pressure was 1×10^{-7} Torr, and during deposition argon gas was used and maintained at a constant pressure of 2 mTorr. In order to avoid any change in deposition conditions, the substrate temperature was maintained

at 3 °C during the deposition process. The average self-bias voltages between the sample and the Si and Mo cathodes were 135.0 ± 0.4 and 85.0 ± 0.3 V, respectively, and their variations were measured during the deposition process: one measurement of the self-bias voltage was performed for each cathode at the beginning of each layer, so that the self-bias voltage evolution could then be monitored. This measurement was performed using a digital voltmeter which was coupled to the cathodes and to the computer that monitors the full process [15]. The influence of the self-bias voltage oscillation on reflectivity and roughness has already been discussed [16]. For the experiments presented in this paper, the self-bias voltage was not adjusted during the deposition process (no regulation) but just measured; however, the RF power was kept at a constant value and the bias voltage oscillations were lower than 0.5%. The theoretical bilayer period which should be realized was 69.1 Å, with a Mo fraction around 0.4, for an optimized reflectivity at near-normal incidence (85°). For all samples, 40 bilayer periods were used. The substrates used were (100)-silicon wafers, ule and zerodur glass ceramic wafers, two inches in diameter, 5 mm thick. Zerodur is a two-phase material that consists primarily of SiO_2 (57%) and Al_2O_3 (25%) but that has eight or nine additional components [12]; ule is a single-phase material consisting of SiO_2 and TiO_2 [17]. The super-polished substrates were produced by SESO[1]. The substrates were cleaned by the manufacturers, but, in addition, they were briefly rinsed with methanol in our laboratory just before deposition.

2.2. Surface characterization

The AFM measurements presented here were conducted on an NT-MDT standalone SMENA-B microscope using the tapping mode. The microscope was fitted with a non-contact ultrasharp silicon cantilever (checked periodically to ensure that it remained sharp) with a typical resonant frequency of 325 kHz. The field sizes were between 5 μm × 5 μm and 1 μm × 1 μm for all AFM scans.

2.3. X-ray scattering and data analysis

A specular and non-specular XRR investigation was performed at near grazing incidence on a conventional two-circle x-ray diffractometer, using a standard fine focus Cu x-ray tube, with a (111)Ge crystal primary beam monochromator to select the Cu Kα_1 radiation. A divergence slit of 50 μm (for specular scans) and 40 μm (for non-specular scans) in front of the monochromator, and a receiving slit of 200 μm, were used. The angular beam divergence was 0.0055°. Specular reflectivity curves were recorded via θ–2θ scans with θ varying from 0° to 8°, and diffuse scattering was measured via ω scans (rocking curves) with 2θ fixed. This provides information about the layer thickness and roughness: the bilayer period and the thickness of each material were determined by fitting SAXRR peaks using the classical matrix thin film method analysis [18–21]. To evaluate the influence of the interfacial roughness, the ideal plane in the ML stack was changed into a rough surface by varying each element in the matrix, i.e. by introducing a Debye–Waller-like attenuation factor which modified the reflectivity coefficients of all interfaces, as extensively described in [21]. The method used allows us to estimate the average height of the roughness of each layer (Mo and Si layers). The calculation program allows us to take into account any shift of the layer thickness and/or the roughness through the stack, but no correction is included to account for the variation of the illuminated area at very grazing angles (however, it is always lower than the sample length).

[1] SESO (Société Européenne de Systèmes Optiques), 305, rue Louis Armand, BP 55000, 13792 Aix-en-Provence Cedex 3, France.

To obtain a complete description of the roughness profile from the substrate up to the surface, including the lateral and vertical correlation lengths, and the fractal dimension of jagged surfaces, non-specular scan analyses (rocking curves) have been performed. The theory used in our rocking-curve analysis is based on the distorted wave Born approximation (DWBA) initially introduced by Sinha *et al* [22] for a single interface and developed for multilayered systems by Holy *et al* [23–26]. In this paper, we only describe the form of the correlation function used for simulations.

It is well known that the surface morphology of growing films commonly shows a fractal appearance, i.e. the film roughness looks the same over many orders of magnification (see, for example, [27]). The interface profile can thus be described by an autocorrelation function $C_j(R)$ (proposed by Sinha):

$$C_j(R) = \sigma_j^2 \exp\left[-\left(\frac{R}{\xi_j}\right)^{2h_j}\right] \tag{1}$$

where σ_j is the rms roughness of the j interface, ξ_j is the lateral correlation length and h_j is the Hurst parameter: h_j is related to the fractal dimension of the surface as $D_j = 3 - h_j$, $0 < h_j \leqslant 1$ [28]. Different values of the Hurst parameter give different interface profiles: small values of h_j define a jagged profile, whereas values approaching 1 define a smooth surface.

However, the calculation of the scattering amplitude requires a knowledge of the roughness correlation function for each interface together with their cross-correlation function $C_{ij}(R)$. Different intermediate approaches assuming partial correlations (i.e. the introduction of a roughness replication factor) have been reported (see, for example, [25, 29, 30]). In our study we used the cross-correlation function suggested by Schlomka *et al* [31, 32], where ξ_v is the vertical correlation length and Z_i and Z_j are the coordinates of the i and j interfaces:

$$C_{ij}(R) = \frac{1}{2}\left[\frac{\sigma_j}{\sigma_i}C_{ii}(R) + \frac{\sigma_i}{\sigma_j}C_{jj}(R)\right]\exp\left(-\frac{|Z_i - Z_j|}{\xi_v}\right). \tag{2}$$

Furthermore, we assume in our simulations that the values of the roughness σ_i, lateral correlation ξ_i and Hurst parameter h_i can change from the first interface (called 'substrate', designated by the subscript '$_S$') to the last interface (i.e. the ML surface called 'ML', designated by the subscript '$_M$'), with a linear variation between the substrate and the surface.

The fitting procedure has been divided into two stages: first, simulations on specular curves allow us to determine the ML period (d), the layer thicknesses (d_{Mo} and d_{Si}), and the substrate and layer average total roughness (σ_S, σ_{Mo} and σ_{Si}). Second, rocking curves on the three first Bragg peaks are analysed simultaneously and the simulation procedure is realized to fit these three curves with the same set of parameters that are: the first and the last interface roughness (σ_S and σ_M), the lateral correlation lengths (ξ_S and ξ_M), the Hurst parameters (h_S and h_M) and the vertical correlation length (ξ_v).

Finally, it should be pointed out that the average roughness determined using specular θ–2θ curves represents the total roughness (σ_{tot}) , whereas the rms roughness extracted from the diffuse scattering analysis represents only the correlated roughness (σ_{cor}). In general, the total roughness includes contributions from vertically uncorrelated roughness (σ_{un} and vertically correlated roughness as follows:

$$\sigma_{tot}^2 = \sigma_{cor}^2 + \sigma_{un}^2. \tag{3}$$

Consequently, the difference between the roughness values estimated from specular curves and diffuse scattering gives information on the roughness correlation.

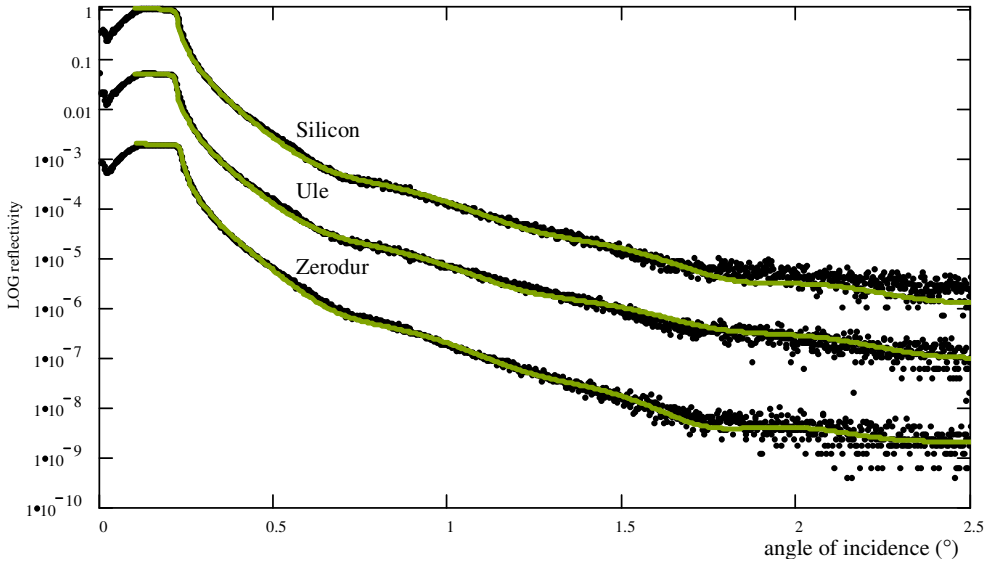

Figure 1. Experimental (dotted curves) and simulated (full curves) SAXRR curves on silicon, ule and zerodur substrates before ML deposition; the simulations are performed with a three-surface layer model.

3. Results and discussion

In this study we have characterized about 20 MLs deposited on silicon, ule and zerodur substrates. Here, we present results obtained on three typical samples that are representative of the results obtained on each substrate type: sample numbers 1, 2 and 3, respectively, deposited on Si, ule and zerodur substrates.

3.1. Characterization of bare substrates (before deposition)

Figure 1 shows both experimental and simulated SAXRR curves corresponding to the three bare substrates before deposition. The three experimental reflectivity curves are similar and reveal specific modulations related to the initial surface state of each substrate (which can be induced by mechanical polishing, chemical etching, oxidation, etc). The scattering observed in the data for incident angles greater than 2° is due to the experimental background noise.

For the simulation, using only the bare bulk-substrate index values, no satisfactory agreement could be obtained to fit the experimental curves, and especially the observed modulations. A more correct fit is obtained using a 'surface-layer' model which modifies the bulk-substrate index near the surface: the introduction of one or more surface layers of uniform density allows us to continuously describe the surface index value variations. Oscillations in the simulated curve appear as soon as a single surface layer is introduced; however, the agreement is bad whatever the angle is. A noticeable improvement is obtained for incident angles lower than 0.5° with a two-'surface-layer' computation, but not for larger angles. It is thus necessary to introduce at least 3 'surface layers' to have a better fit with the experimental curve modulations. However, this may not be a true representation of what is happening (as is known, several possibilities can give a good fit): this 'surface-layer' approach reflects only a continuous change in the substrate optical index near the surface. Figure 2

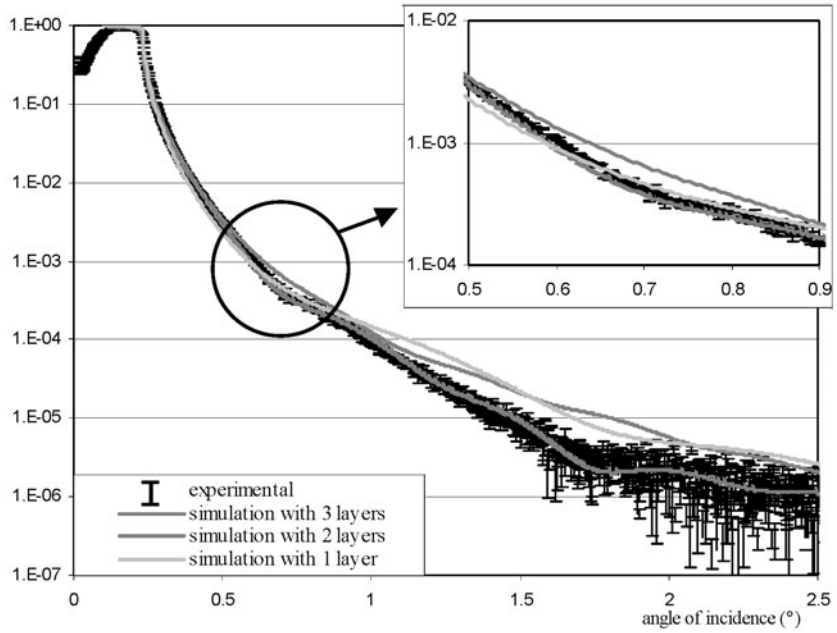

Figure 2. Experimental and simulated SAXRR spectra on a zerodur substrate before deposition; the simulations are performed with 1, 2 and 3 'surface layers' on the substrate.

Table 1. Substrate characteristics introduced in SAXRR simulations performed on substrates before deposition; n and k are related to the optical index ($\tilde{n} = n + ik$), N is the number of surface layers introduced; e_1, e_2 and e_3 are, respectively, the thickness values of the first, second and third surface layer (from the substrate up to the surface); e_T is the total thickness of these layers and σ is the surface roughness.

Substrate	n	k	N	e_1	e_2	e_3	e_T (Å)	σ (Å)
Silicon	7.59×10^{-6}	1.73×10^{-7}	3	35	24	14	73	4.0 ± 0.4
Ule	7.183×10^{-6}	1.119×10^{-7}	3	32	30	16	78	3.0 ± 0.6
Zerodur	8.41×10^{-6}	1.11×10^{-7}	3	37	25	12	74	5.6 ± 0.6

shows the improvement in fit as a function of the number of surface layers introduced in the model for the zerodur substrate (in the inset the misfit for a two-layer model is shown). The parameters used to obtain the best fit for each substrate type are given in table 1. With regard to these parameters, the calculations suggest that the zerodur substrate has a greater surface roughness than the others. This could explain the noticeable decrease in the SAXRR intensity observed in figure 1 for angles greater than 1.8°.

AFM images obtained on the three substrate types are presented in figure 3. These images concern a surface area of 10×10 μm^2. Globally, ule and Si substrates exhibit very similar surface states with comparable rms roughness values (respectively 1 and 1.2 Å); on the other hand, the average rms roughness of zerodur substrates is more than twice as high (2.5 Å). The use of the AFM technique, which is more sensitive to the surface state than SAXRR, allows us to deduce that the surface treatments performed on these different substrates, even if similar, lead to a higher roughness value in the case of a zerodur substrate, as already suggested by the SAXRR results.

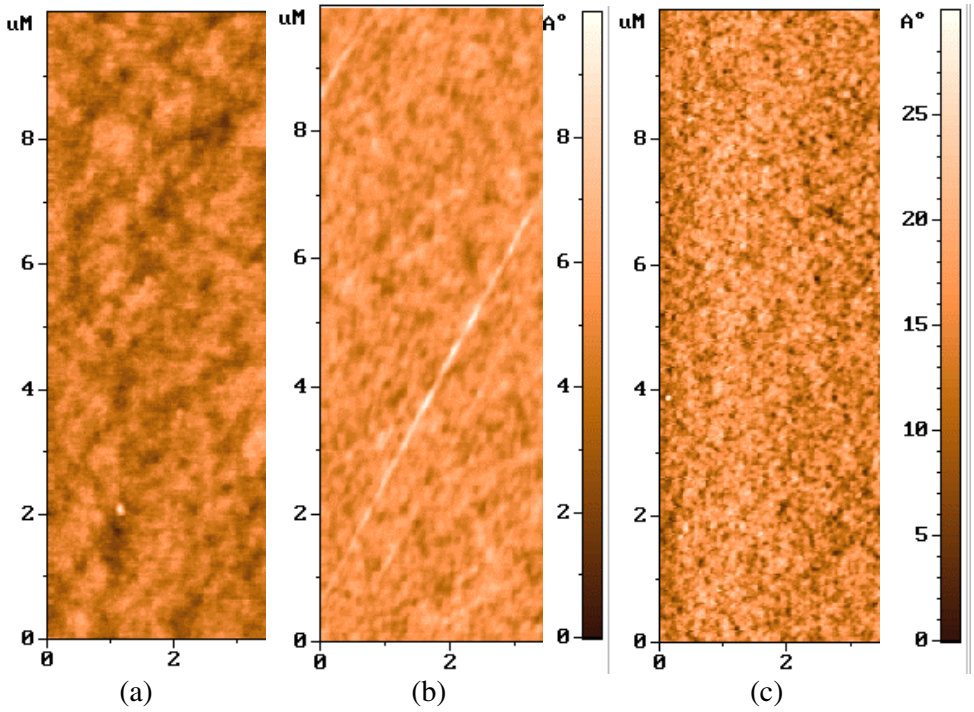

Figure 3. Part of 10×10 μm^2 AFM images of substrate surfaces before deposition; (a) silicon substrate, the colour scale varies between 0 and 10 Å, $\sigma_{rms} = 1.1 \pm 0.4$ Å; (b) ule substrate, the colour scale varies between 0 and 10 Å, $\sigma_{rms} = 0.9 \pm 0.4$ Å; (c) zerodur substrate, the colour scale varies between 0 and 30 Å, $\sigma_{rms} = 2.7 \pm 0.3$ Å.

3.2. After-deposition characterization

Specular SAXRR of MLs 1, 2 and 3 are shown in figure 4. This figure also presents the simulated curves for the three samples.

For MLs deposited on Si and ule substrates (numbers 1 and 2), the first ten Bragg peaks distinctly appear and are not broadened. This clearly proves that there is no visible layer thickness evolution through the ML, from the substrate up to the surface: in fact, a shift in the period value due to any modification in the deposition conditions should broaden the last Bragg peak. Moreover, as high-order Bragg reflections are strongly suppressed by interface roughness, the sharpness and the intensity of these ten Bragg maxima indicate that the interfaces are undoubtedly smooth.

For sample 3 deposited on a zerodur substrate, the Bragg peaks disappear for incidence angles greater than 5°, in accordance with higher interface roughness values.

For these three samples, the periods of which are very close, SAXRR simulation results are reported in table 2(a). The simulations also provide an evaluation of the average roughness for the substrate and for the Si and Mo layers. These values are very similar for MLs 1 and 2 deposited on Si and ule substrates, but they are globally higher in the case of sample 3 (zerodur substrate). As observed in other studies [11, 33], a higher ML total roughness is obtained when the substrate roughness is higher. Table 2(a) also shows that, whatever the sample is, the Si roughness is lower than the Mo roughness; this result has already been discussed [16] and is related to the difference in the stability of self-bias voltage for the Mo and Si cathodes during the deposition process.

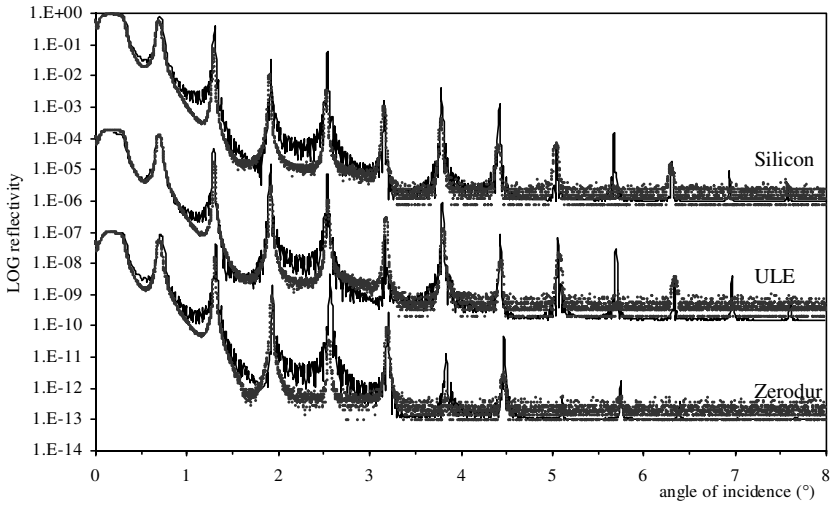

Figure 4. Specular SAXRR measurements (dotted curves) on MLs deposited on silicon, ule and zerodur substrates; the simulated data are also shown (full curves).

Table 2. Sample characteristics introduced in both specular (a) and non-specular (b) SAXRR simulations. In the case of specular simulations, σ is the average total roughness height, the subscript 's' refers to the substrate, d, d_{Si} and d_{Mo} are the bilayer, Si layer and Mo layer thickness values, respectively. In the case of rocking-curve simulations, σ is the average correlated roughness height, the subscripts 'S' and 'M' refer to the substrate and the surface, respectively, h is the Hurst parameter and ξ and ξ_v are the lateral and vertical correlation lengths.

Sample substrate	Number 1 (silicon)	Number 2 (ule)	Number 3 (zerodur)
(a) Data deduced from specular SAXRR simulations			
d (Å)	70.2 ± 0.1	69.8 ± 0.1	69.3 ± 0.1
d_{Mo} (Å)	27.0 ± 0.2	28.6 ± 0.2	25.0 ± 0.2
d_{Si} (Å)	43.2 ± 0.2	41.2 ± 0.2	44.3 ± 0.2
σ_s (Å)	2.7 ± 0.2	2.6 ± 0.3	3.0 ± 0.3
σ_{Mo} (Å)	2.7 ± 0.4	2.6 ± 0.3	2.9 ± 0.5
σ_{Si} (Å)	2.2 ± 0.3	2.0 ± 0.4	2.6 ± 0.4
(b) Data deduced from rocking-curve simulations			
σ_S (Å)	1.3 ± 0.2	0.95 ± 0.05	2.2 ± 0.1
σ_M (Å)	0.85 ± 0.15	0.65 ± 0.05	2 ± 0.1
h_S	0.15 ± 0.05	0.25 ± 0.02	0.6 ± 0.02
h_M	0.1 ± 0.02	0.15 ± 0.05	0.5 ± 0.02
ξ_S (Å)	400 ± 90	200 ± 50	300 ± 100
ξ_M (Å)	350 ± 90	100 ± 50	250 ± 50
ξ_v (Å)	17.5 ± 2.5	15 ± 2	90 ± 2

Since a complete analysis of the roughness needs a diffuse scattering study, figures 5 and 6 show simulated and experimental rocking curves recorded on the first three Bragg peaks for samples 2 (ule substrate) and 3 (zerodur substrate), respectively. In both cases, the simulations are in good agreement with the experiments. Due to their great similarity with the results of sample 2, the rocking curves of sample 1 (Si substrate) are not presented.

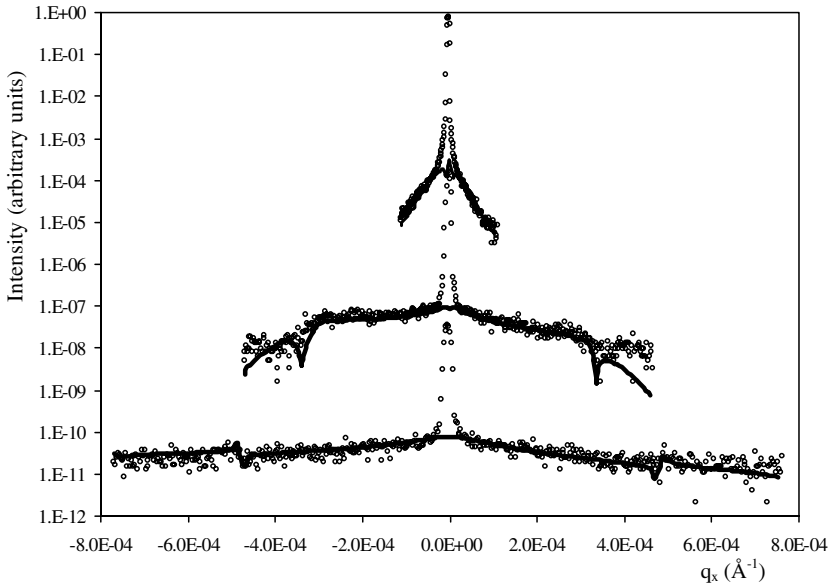

Figure 5. Experimental (○) and simulated (full curves) rocking curves for the first three Bragg peaks in the case of ML 2 deposited on a ule substrate.

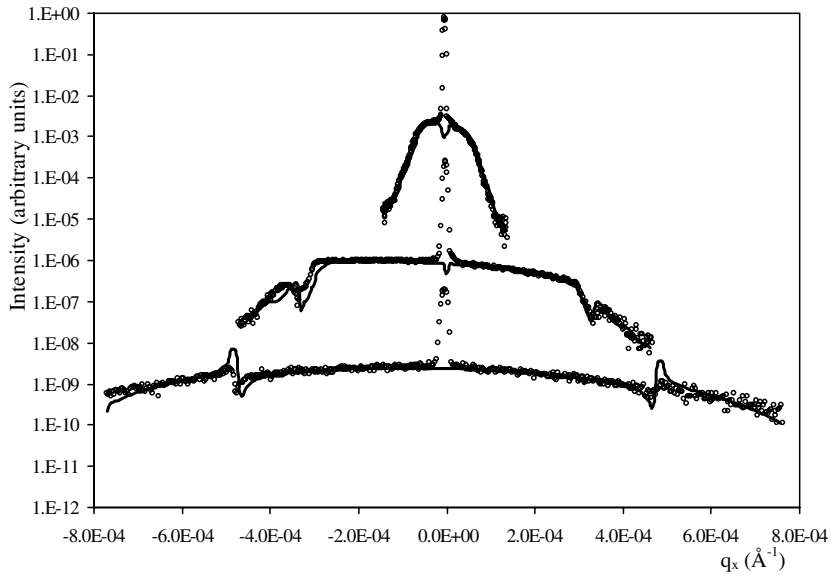

Figure 6. Experimental (○) and simulated (full curves) rocking curves for the first three Bragg peaks in the case of ML 3 deposited on a zerodur substrate.

First of all, it is clear that the diffuse scattering intensity level is more significant for sample 3 (zerodur) than for sample 2 (ule): this is the manifestation of a higher imperfection level for the interfaces of sample 3. The roughness characteristics deduced from the rocking-curve simulations are reported in table 2(b) for the three samples. These results indicate that the correlated roughness, as well as the vertical correlation length and the Hurst parameter,

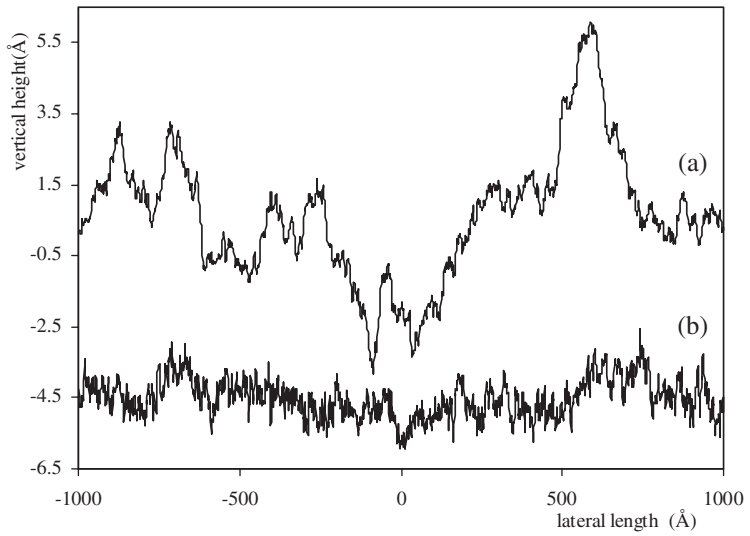

Figure 7. Simulation of the ML surface profile using rocking-curve simulation parameters in the case of (a) sample 2 deposited on a ule substrate and (b) sample 3 deposited on a zerodur substrate; curve (b) has been intentionally moved forward.

are more important for sample 3 (on a zerodur substrate) ($\sigma_M \approx 2$ Å, $\xi_v = 90$ Å, $h = 0.6$ Å) than for samples 1 and 2 ($\sigma_M < 1$ Å, $\xi_v < 20$ Å, $h < 0.3$ Å). However, lateral correlation lengths are rather similar for all three samples. This means that, in the case of a ule or a Si substrate, the roughness attenuation is rapid as its replication is not significant and, if $\xi_v < 20$ Å, the roughness replication does not persist over more than four or five layers. In the case of a zerodur substrate, the roughness, whose average height is more important, is repeated over about 15 layers. Moreover, it is well worth noting that the value of the ML roughness (σ_M) is lower than that of the substrate (σ_S), independently of the type of substrate. All these results show that, for the roughness frequencies measured by SAXRR (i.e. HSFR), the film surface roughness does not depend upon that of the substrate. This result, previously shown in [16], confirms that, in general, a film deposited using magnetron sputtering presents a reduced roughness in comparison with that of the substrate (at high spatial frequencies). This is in accordance with the results obtained by Freitag and Clemens [27]. This smoothing effect could be due to the amorphous Si layers, which could smooth the cumulative roughness intrinsic to polycrystalline Mo growth [27]. Furthermore, this effect, measured by SAXRR, is also in accordance with the results of Savage *et al* [34] who suggested that the interfaces act towards preferentially smoothing the high-frequency components of the roughness, whereas the long-wavelength components can be replicated through the ML stack (implying in that case an increase of the lateral correlation length).

Secondly, one can notice that, when the average roughness height is very low (<1.5 Å), the Hurst parameter is very close to zero (<0.2 for the ML surface) implying high spatial frequency oscillations (see section 2.3); conversely, when the roughness is higher (>2 Å), the Hurst parameter is increased (>0.5). Figure 7 presents the surface profile simulations performed with the parameters of table 2(b) for samples 2 (ule) and 3 (zerodur). The high spatial frequency fluctuations are clearly visible for the ML deposited on a ule substrate. Consequently, we may conclude that, in our experiments, when the roughness is small, the surface expresses mainly high spatial frequency fluctuations. This is not the case when the roughness is more important.

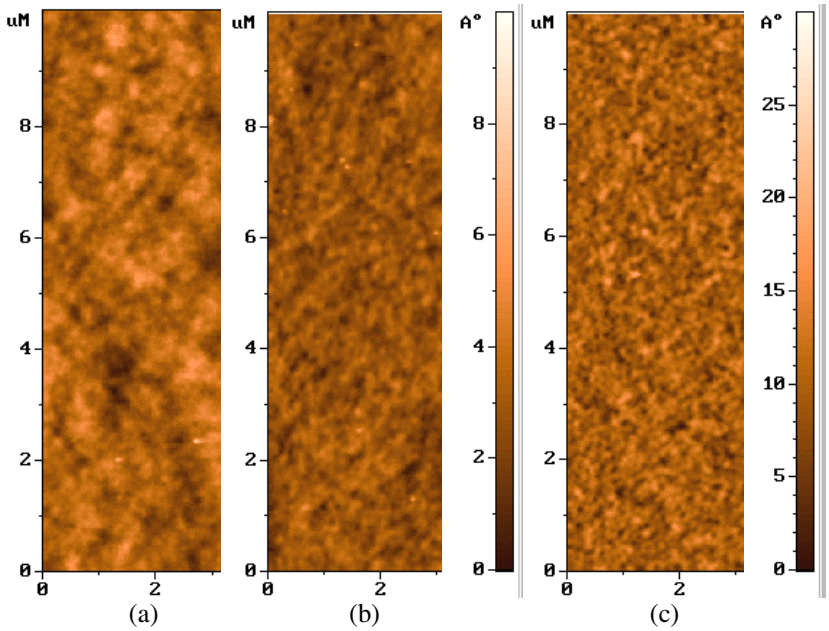

Figure 8. Part of $10\times10\,\mu\mathrm{m}^2$ AFM images recorded after the deposition of MLs; (a) ML 1 deposited on a Si substrate, the colour scale varies between 0 and 10 Å, $\sigma_{rms} = 1.0\pm0.4$ Å; (b) ML 2 deposited on a ule substrate, the colour scale varies between 0 and 10 Å, $\sigma_{rms} = 0.7 \pm 0.4$ Å; (c) ML 3 on a zerodur substrate, the colour scale varies between 0 and 30 Å, $\sigma_{rms} = 2.2 \pm 0.3$ Å.

Finally, using equation (3), one can evaluate the average uncorrelated roughness (σ_{un}) of the film deposited using magnetron sputtering. In fact, specular and non-specular measurements allow us to respectively separate the total roughness (σ_{tot}, deduced from specular simulations) and the correlated roughness (σ_{cor}, deduced from rocking-curve simulations). For the layer, the average correlated roughness is taken equal to σ_M in table 2(b) and the total roughness is taken equal to the average of σ_{Mo} and σ_{Si} in table 2(a). Such an evaluation of σ_{un} shows that, regardless of the ML and the substrate type, $\sigma_{un} = 2.1 \pm 0.2$ Å.

This value is low and corresponds to the intrinsic roughness due to the deposition technique in relation to the deposited material. In the case of Mo/Si MLs deposited on zerodur substrates using a direct-current (DC) magnetron sputtering system, Mirkarimi *et al* [11] have estimated the intrinsic roughness of the ML interfaces to be approximately 1.3 Å. However, to obtain this value, the authors have analysed the ML and substrate *surface* roughness using AFM characterization, whereas we determined the intrinsic roughness by analysing the interface roughness of the whole ML using SAXRR. The two results cannot therefore be directly compared.

AFM images taken after deposition are shown in figure 8. For all substrates, the final rms surface roughness is lower than its value before deposition. This result is in good agreement with the SAXRR results. For comparison, figure 9 shows the rms roughness measured on a $2.5 \times 2.5\ \mu\mathrm{m}^2$ surface area before and after deposition. As the usual roughness requirement for EUV optics is to be less than 1 Å at this scale, it is clear that zerodur substrates, which present a typical roughness of more than 2 Å, should not be retained for film deposition, even if this value is low. To go further in the comparison of the AFM and SAXRR results, figure 10 shows line scans of the ML surface profile; these line scans are extracted from $0.5 \times 0.5\ \mu\mathrm{m}^2$ AFM pictures taken on the surfaces of samples 2 and 3. This figure, which can be compared

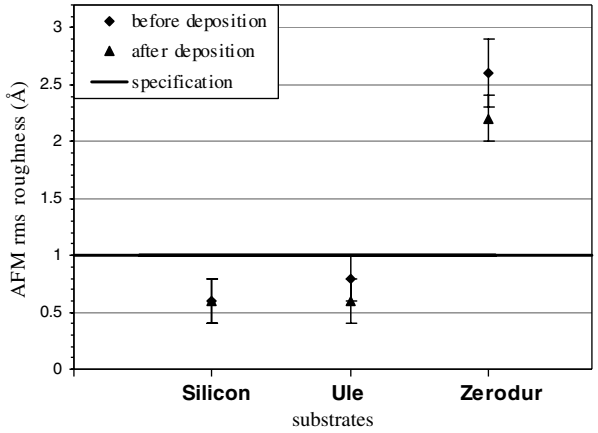

Figure 9. Rms roughness before and after deposition deduced from AFM measurements realized on a 2.5×2.5 μm^2 surface area.

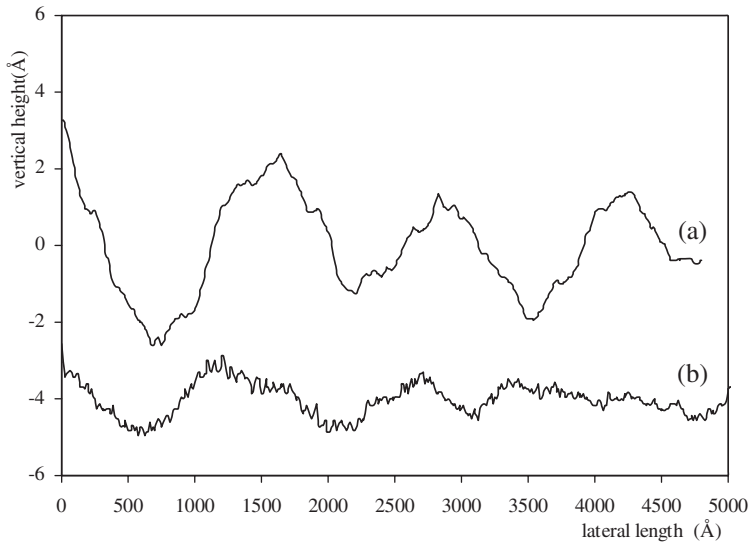

Figure 10. Line scans of the surface profile extracted from AFM 0.5×0.5 μm^2 pictures recorded on ML surfaces: (a) surface of sample 2 deposited on a ule substrate, (b) surface of sample 3 deposited on a zerodur substrate. Curve (b) has been intentionally moved forward.

with figure 7, shows that HSFR oscillations are more important for a ule substrate (sample 2) than for a zerodur substrate (sample 3). The results deduced from the rocking-curve analyses (see figure 7) are thus qualitatively confirmed by the AFM technique. However, although the two techniques are qualitatively in good agreement, it is difficult at this point to quantitatively compare the two results. Actually, 10×10 μm^2 AFM scans (figures 3 and 8) are mainly related to middle spatial frequency roughness (MSFR, $f < 1$ μm^{-1}), and AFM scan areas lower than 5×5 μm^2 concern both the MSFR and HSRF. On the other hand, our SAXRR results are only related to HSRF ($f < 1$ μm^{-1}): for example, the maximal spatial frequency that is analysed in our rocking-curve experiments is about 20 μm^{-1} for the third-order Bragg peak. Thus, the differences between the roughness values evaluated by AFM and SAXRR

could also be explained by the differences between the spatial frequency ranges of the two techniques. Thus, in order to perform a quantitative comparison of both roughness results, it is necessary to evaluate the rms roughness according to the spatial frequency (with the power spectral density analysis).

For technical applications, the results concerning Si and ule substrates renders them more advantageous for the EUV mirror deposition. However, considering the conditions of use, ule substrates would be preferable owing to their low thermal expansion value.

4. Conclusion

We have studied the influence of the substrate quality and the deposition technique on the propagation and value of the ML roughness, by combining specular and non-specular SAXRR and AFM techniques. The results show that, whatever the substrate roughness is, the deposition process smooths the film, so that the final roughness is always lower than the initial one. Moreover, the rocking-curve simulation data give us access to important parameters such as the vertical correlation length, the Hurst parameter and the average correlated roughness of the substrate and the ML surface. These results show that, for Si and ule substrates, the average roughness height is very low ($\sigma < 1.5$ Å), associated with high-spatial-frequency oscillations ($h < 0.2$), whereas in the case of a zerodur substrate, the roughness value is significantly increased ($\sigma > 2$ Å), and the high-spatial-frequency oscillations are reduced ($h > 0.6$). These parameters concern, in fact, each interface in the ML and are thus important for the EUV optics. Although the real influence of such fluctuations on EUV imaging processes is not quite clear at present, it seems preferable to have an average roughness lower than 2 Å as the technical requirements always impose the lowest roughness values. In these conditions, and taking into account our results, Si and ule substrates can be considered as the best candidates for EUV optics, as compared with zerodur substrates. However, it is important to note that the Si thermal expansion coefficient is not small enough to prevent harmful thermal effects.

The combination of specular and non-specular SAXRR results leads to the evaluation of another key parameter, the uncorrelated roughness, which is an intrinsic characteristic related to both the chosen deposition technique and the material. In our case, using RF-magnetron sputtering and Si and Mo materials, we find a characteristic intrinsic roughness of 2 Å. This value is very low and constitutes a good argument in favour of the use of this technique for EUV mirror deposition.

The roughness values evaluated by SAXRR and AFM are similar. However, for further study of the correlation between the roughness values evaluated by these techniques, one needs to use the power spectral density analysis in order to correctly compare the rms roughness value with that of the spatial frequency roughness. This work is in progress.

References

[1] Gwyn C W, Stulen R H, Sweeney D W and Attwood D 1998 EUV lithography *J. Vac. Sci. Technol.* B **16** 3142–9
[2] Taylor J S, Sommargren G E, Sweeney D W and Hudyma R M 1998 *Proc. SPIE–Int. Soc. Opt. Eng.* **3331** 580–90
[3] Sweeney D W, Chapman H N, Hudyma R M and Shäfer D R 1998 EUV optical design for a 100 nm CD imaging system *Emerging Lithographic Technologies II (Proc. SPIE vol 3331)* ed Y Vladirmirsky pp 2–10
[4] Stearns D G, Rosen R S and Vernon P 1991 *J. Vac. Sci. Technol.* A **9** 2662
[5] Tenant D M, Bjorkholm J E, D'Souza R, Eichner L, Freeman R R, Pastalan J Z, Szeto L H, Wood O R II, Jewell T E, Mansfield W M, Waskiewics W K, White D L, Windt D L and MacDowell A A 1991 *J. Vac. Sci. Technol.* B **9** 3176
[6] Stearns D G, Gaines D P and Sweeney D W 1998 *J. Appl. Phys.* **84** 1003–28

[7] Nguyen K B and Nguyen T D 1993 *J. Vac. Sci. Technol.* B **11** 2960–2970
[8] Hue J, Muffato V, Pellé C, Quesnel E, Garrec P and Baume F 2001 *Proc. SPIE–Int. Soc. Opt. Eng.* **4343** 627–38
[9] Burkhart S, Cerjan C, Kearney P, Mirkarimi P and Walton C 1999 Low-defect reflective mask blanks for extreme ultraviolet lithography *Part of the SPIE Conf. on Emerging Lithographic Technologies III vol 3676* pp 570–7
[10] Pistor T, Deng Y F and Neureuther A 2000 Extreme ultraviolet mask defect simulation: low-profile defects *J. Vac. Sci. Technol.* B **18** 2926–9
[11] Mirkarimi P B, Bajt S and Wall M A 2000 *Appl. Opt.* **39** 1617–25
[12] Bach H 1995 *Low Expansion Glass Ceramics* (Heidelberg: Springer)
[13] Mirkarimi P B, Baker S L, Montcalm C and Folta J A 2001 *Appl. Opt.* **40** 62–70
[14] Vidal B and Marfaing J 1991 *Opt. Eng.* **30** 636
[15] Cilia M, Yakschin A, Trambly H, Vidal B and Bretagne J 1998 *Thin Solid Films* **312** 320–6
[16] Putero-Vuaroqueaux M and Vidal B 2001 Extreme ultraviolet multilayer mirrors deposited using radio-frequency-magnetron sputtering: the influence of self bias voltage on reflectivity and roughness *J. Phys.: Condens. Matter* **13** 3969–76
[17] Gulati S T 1992 Mechanical properties of SiO_2 vs SiO_2–TiO_2 bulk glasses and fibers *Optical Waveguide Materials* vol 244, ed M M Broer, G H Siegel, R T Kersten and H Kawazoe (Pittsburgh, PA: Materials Research Society) pp 67–84
[18] Parrat L G 1954 *Phys. Rev.* **95** 359
[19] Névot Louis 1978 *PhD Thesis* Université de Paris-Sud, Centre Orsay
[20] Lee P 1981 *Opt. Commun.* **37** 159
[21] Vidal B and Vincent P 1984 *Appl. Opt.* **23** 1794
[22] Sinha S K, Sirota E B, Garoff S and Stanley H B 1988 *Phys. Rev.* B **38** 2297
[23] Holy V, Kubena J, Ohlidal I, Lisckla K and Plotz W 1993 *Phys. Rev.* B **47** 15 896
[24] Wong P Z and Bray A 1989 *Phys. Rev.* B **37** 7751
[25] Holy V and Baumbach T 1994 *Phys. Rev.* B **49** 10 668
[26] Holy V, Pietsch U and Baumbach T 1998 *X-ray Scattering by Thin Films and Multilayers* (Berlin: Springer)
[27] Freitag J M and Clemens B M 2001 *J. Appl. Phys.* **89** 1101–7
[28] Mandelbrodt B B 1982 *The Fractal Geometry of Nature* (New York: Freeman)
[29] Kaganer V M, Stepanov S A and Kölher R 1996 *Physica* B **221** 34
[30] Ming Z H, Krol A, Soo Y L, Kao Y H, Park J S and Wang K L 1993 *Phys. Rev.* B **47** 16 373
[31] Trambly de Laissardière H 1997 Etude de miroirs multicouches X en réflexion et lumière diffuse. Application à l'analyse des multicouches implantées et à la fabrication d'optique diffractive *PhD Thesis* University of Aix-Marseille III
[32] Schlomka J P, Fitzsimmons M R, Pynn R, Stettner J, Seeck O H, Tolan M and Press W 1996 *Physica* B **221** 44
[33] Ulyanenkov A, Matsuo R, Omote K, Inaba K, Harada J, Ishino M, Nishii M and Yoda O 2000 *J. Appl. Phys.* **87** 7255–60
[34] Savage D E, Shimke N, Phang Y H and Lagally M G 1992 *J. Appl. Phys.* **71** 3283